

Critical dynamics of superconducting BSCCO films

K. D. Osborn* and D. J. Van Harlingen, Vivek Aji, Nigel Goldenfeld, S. Oh and J. N. Eckstein

*Department of Physics,
University of Illinois at Urbana-Champaign
1110 West Green Street
Urbana, IL, 61801-3080*

(Dated: December 2, 2024)

We report on a systematic investigation of the critical fluctuations in the complex conductivity of epitaxially-grown $\text{Bi}_2\text{Sr}_2\text{CaCu}_2\text{O}_{8+\delta}$ films for $T \lesssim T_c$ using a two-coil inductive technique at zero applied field. We observe the static 3D-XY critical exponent in the superfluid density near T_c . Linear scaling analysis close to the critical temperature yields a dynamic critical exponent of $z = 2.0$ for small drive currents, but non-linear effects are seen to be important. At T_c , a non-linear scaling analysis also yields a 3D dynamic exponent of $z = 2.0$.

PACS numbers: 74.40.+k, 74.25.Nf, 74.72.Hs, 74.76.Bz

Direct observation of the scaling properties of the superconducting transition has at last become feasible due to the discovery of the cuprate superconductors. Microwave measurements in $\text{YBa}_2\text{Cu}_3\text{O}_{7-x}$ (YBCO) have provided strong evidence that for accessible temperature ranges, the effective static universality class is the three dimensional XY model (3D-XY)[1]. Transport measurements have probed the dynamics of the critical fluctuations, which are characterized by the value of the dynamic critical exponent z describing how the relaxation time τ scales with the correlation length ξ : $\tau \sim \xi^z$. However for YBCO, experiments have not yielded a consistent picture. For example, longitudinal dc-resistivity measurements yield $z = 1.5 \pm 0.1$ [2] at small but finite magnetic field while microwave conductivity measurements are consistent with $z = 2.3 - 3.0$ [3].

Critical fluctuation results on $\text{Bi}_2\text{Sr}_2\text{CaCu}_2\text{O}_{8+\delta}$ (BSCCO) are even more dissimilar. In previous work on BSCCO crystals a non-linear transport study found 2D critical behavior with an anomalous dynamic exponent of $z \approx 5.6$ and no crossover to 3D behavior [4]. The 3D universal phase angle of the complex conductivity deduced from the magnetic susceptibility of BSCCO yields an even larger value of z [5]. However, the complex conductivity of underdoped BSCCO measured at terahertz frequencies agrees with a Kosterlitz-Thouless-Berezinskii (KTB) model with diffusive dynamics [6, 7]. Only dc fluctuation conductivity measurements in BSCCO find relaxational dynamics, $z \approx 2.0$, assuming a 3D-XY static exponent, $\nu \approx 2/3$ [8], in agreement with this paper and recent theoretical work that predicts that $z \approx 2.0$ in 3D [9]. While a larger value of the dynamic exponent ($z > 2$) can be understood as disorder effects, only the presence of a previously undetected collective mode coupled to the superfluid density would lead to $z \approx 1.5$ in 3D, just as occurs in superfluid He^4 [10].

In this paper we provide results on the critical fluctuations in epitaxially-grown BSCCO films. We have measured the ab-plane complex conductivity with a two-coil inductive technique at zero applied magnetic field ($H = 0$). Our measurements indicate that the critical fluctuations in BSCCO films are consistent with the 3D-XY critical fluctuation model, rather than a KTB transition within the layers. This contrasts with previous studies using this technique on YBCO, which report KTB critical [11] and mean-field [12] fluctuations. Analysis of the phase angle of the film response, using the linear response theory in the critical region, yields a dynamic exponent of $z = 2.0$. However, the breakdown of linear response theory becomes important near the transition temperature T_c and the analysis is complicated by the need to extract the superfluid density from the measured mutual inductance by an approximate inversion technique. Our analysis shows that the determination of z purely from linear response theory is contaminated by non-linear effects, and at probe currents that are too large the effective value of z inferred can be as low as 1.5. To circumvent this problem we derive a non-linear scaling law obeyed by the raw measured mutual inductance at T_c (i.e. without the need for a data inversion) and extract the dynamic exponent directly from the data. In agreement with the linear response analysis, we again obtain $z = 2.0$.

Experimental setup: We have measured several high quality oxygen-doped BSCCO films, grown by molecular-beam-epitaxy on SrTiO_3 substrates and analyzed in-situ by RHEED [13]. The BSCCO films are nominally oriented along the c-axis, with unit cell thickness of $d = 15.4$ Å. Films A, B, and C have $n = 21, 40$ and 60 unit cells respectively and are grown on 10 and 14 mm square substrates. Film A is overdoped, while film B and C are slightly overdoped and underdoped, respectively.

To obtain the ab-plane complex conductivity, we employ a two-coil inductive technique. The mutual inductance of two coaxial coils is measured with a film placed in between and normal to the axis of the coils. An ac current is applied through the drive coil; a second coil,

*Present address: National Institute of Standards and Technology, Boulder, CO, 80305

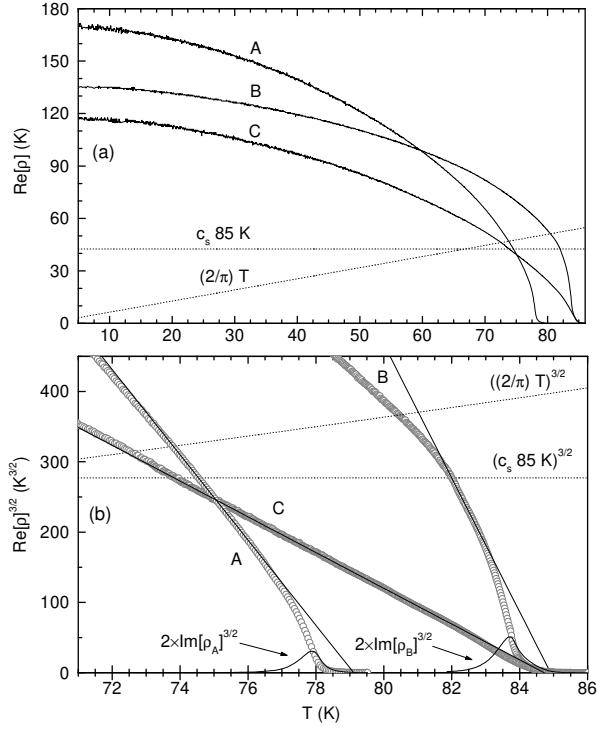


FIG. 1: $Re[\rho]$ (panel a) and $Re[\rho]^{3/2}$ (panel b), as a function of temperature for films A through C. $\rho = (c_s 85 K)$ is the predicted crossover to 3D-XY critical behavior and $\rho = (2/\pi)T$ is the KTB critical superfluid density for an isolated bilayer.

attached to a large input impedance lock-in amplifier, measures the fields produced by the drive coil and the screening currents in the film. The coils have 135 turns and an average radius of 1.5 mm. The drive coil is placed 0.35 mm above the film so that at a current of $I = 50 \mu A$ rms the applied ac magnetic field is < 0.1 Gauss normal to the film. Measurements are performed in a He^4 continuous-flow dewar, which allows the temperature of the film to be controlled without significant heating from the drive coil. The sample temperature is monitored by a Si diode attached to the back side of the substrate.

Complex conductivity and superfluid density: The complex conductivity $\sigma = \sigma_1 - i\sigma_2$ of each film is calculated from the mutual inductance using the exact analytical expression for an infinite diameter film [14] and a numerical inversion technique similar to that of Fiory *et al.* [15]. The method of Turneaure *et al.* [16] is employed to correct for film diameter effects prior to calculating the in-plane complex conductivity. The measured penetration depth $\lambda_{ab} = (\mu_0 \omega \sigma_2)^{-1/2}$, is independent of the measurement frequency from $f = 10 - 100$ kHz below the transition temperature, where the dissipation is small ($\sigma_1 \ll \sigma_2$). To analyze the critical fluctuations, we study the complex superfluid density per CuO bilayer, $\rho = i\sigma \omega d \Phi_0^2 / (4\pi^2 k_B)$, where Φ_0 is the superconducting flux quantum [17]. The real part of this quantity, $Re[\rho]$ has units of temperature and sets the energy scale for crit-

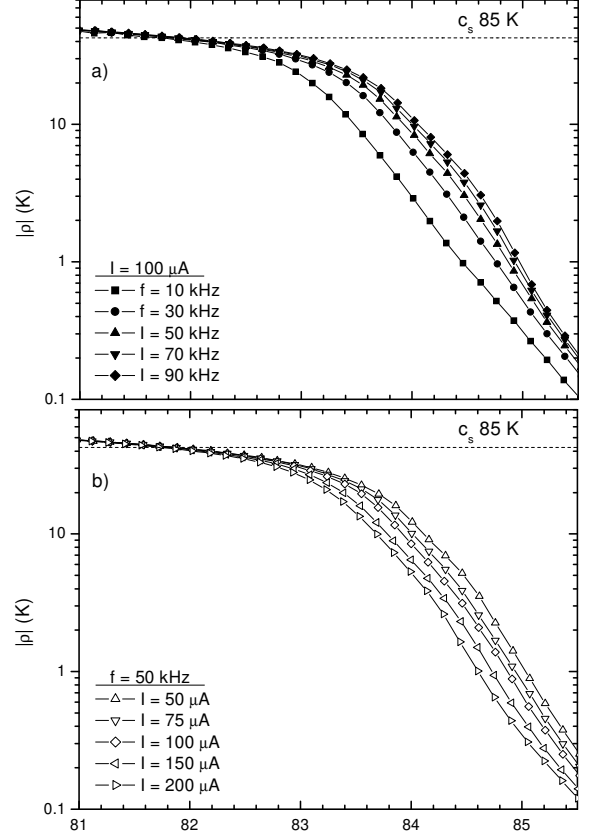


FIG. 2: $|\rho|$ in film B taken at a series of frequencies (panel a) and drive currents (panel b).

ical fluctuations. In Fig. 1(a) $Re[\rho]$ is plotted for films A through C, obtained at $f = 80$ kHz and $I = 40 \mu A$. At 5 K, films A, B, and C, have penetration depths of 235, 265, and 285 nm, respectively. The low temperature doping and temperature dependence will be discussed elsewhere.

Static critical fluctuations: The mean field behavior, expected at low temperatures, crosses over to the 3D-XY behavior as the critical temperature is approached from below. In layered systems, the 3D-XY behavior is exhibited once the c-axis correlation length exceeds the interlayer spacing, d ; i.e. when $\rho(T) = c_s T_c$, where $c_s \approx 0.5$ and $\rho = Re[\rho]$ [1]. In Fig. 1(b), the data from Fig. 1(a), are plotted as $Re[\rho]^{3/2}$ near the critical regime. Also shown in Figs. 1(a) and 1(b) is the corresponding power of $c_s T_c$ to locate the onset of 3D-XY behavior. The static 3D-XY model gives $\rho \sim \xi^{-1} \sim |T - T_c|^\nu$, where $\nu \approx 2/3$. We observe that $Re[\rho]^{3/2}$ varies linearly in temperature for $\rho(T) \lesssim c_s T_c$ indicating a 3D-XY, rather than mean-field ($\rho \sim |T - T_c|$), behavior. In addition, this behavior is independent of measurement frequency and current. In film C the linear regime is as large as 7 K below 82 K. The linear fits extrapolate to estimates of $T_c = 79.1$ K, 84.9 K and 84.7 K for films A, B and C respectively.

Dimensional crossover: In Figs. 1(a) and 1(b) a power of $2T/\pi$ is shown to locate where we would ex-

pect the KTB transition for a noninteracting bilayer, $\rho = 2T/\pi$ [18]. We observe no drop in the superfluid density at this temperature in our films. The films instead exhibit three dimensional behavior with coupling among the bilayers, precluding a KTB transition in the bilayers. At a higher temperatures we do observe a drop in the superfluid density from the static scaling value which may be interpreted as a crossover to two dimensional behavior. We do not believe this to be the case in our films since the drop is observed to be current as well as frequency dependent (see figure 2). Notice that the superfluid density does drop more rapidly than expected from the 3DXY model as the frequency is decreased for a given drive current, but does so more slowly as the current is decreased at fixed frequency. While the former would lead one to conclude that 3DXY behavior is not valid in the static limit, the latter would imply the opposite. More accurate measurements are needed at low frequency and currents to establish unambiguously the true nature of the static limit. Nevertheless the trend with decreasing current, coupled with the phase angle dependence discussed in the next section, is consistent with 3DXY behavior. The crossover to 2D behavior is expected when ξ_c becomes as large as the film thickness, h . 3D-XY scaling implies that this occurs at a temperature, T^* , which is 0.05 K, 0.01 K and 0.02 K below the transition temperature for films A, B and C respectively. This implies that the region of pure 2D fluctuations is too small to be resolved in our data and therefore we expect 3D fluctuations to dominate.

Dynamic critical fluctuations: Next we study the phase of ρ , ϕ_ρ , close to the transition temperature. The frequency dependence of $2\phi_\rho/\pi$ for film B measured at $I = 100 \mu A$ is shown in Fig. 3(a). Within linear response theory, the phase angle is independent of frequency at the critical temperature and is given by $\phi_\rho(T_c) = \pi/(2z)$ in three dimensions, where z is the dynamic critical exponent [19]. In Fig. 3(a) we notice that the curves for different frequencies seem to approach a phase angle consistent with a dynamic exponent of $z \approx 1.5$ and $T_c = 84.9$ K. When repeated at a smaller value of the current, $I = 50 \mu A$, $\phi_\rho(T_c)$ is smaller, as shown. Since the constant phase angle is a result from linear response theory, the estimate of the dynamic exponent from the data is expected to be more accurate at smaller currents.

This is indeed seen in the current dependence of the phase angle at different frequencies for film C. In Fig. 3(b), $2\phi_\rho/\pi$ is shown for a set of frequencies and currents. As the current is lowered, the frequency independent phase angle shifts to lower values. At $20 \mu A$, $10 \mu A$ and $5 \mu A$, this phase angle is $0.57\pi/2$, $0.54\pi/2$ and $0.51\pi/2$ respectively. Extrapolation to $I = 0$, yields a bulk critical exponent of $z = 2.0$ and $T_c = 85.8$ K. This suggests that the result of $z \approx 1.5$ from film B is an artifact of the large current used in the measurement. With this analysis, the thickest film (C) exhibits a critical phase angle, the film with intermediate thickness (B) provides evidence for similar behavior, but the thinnest

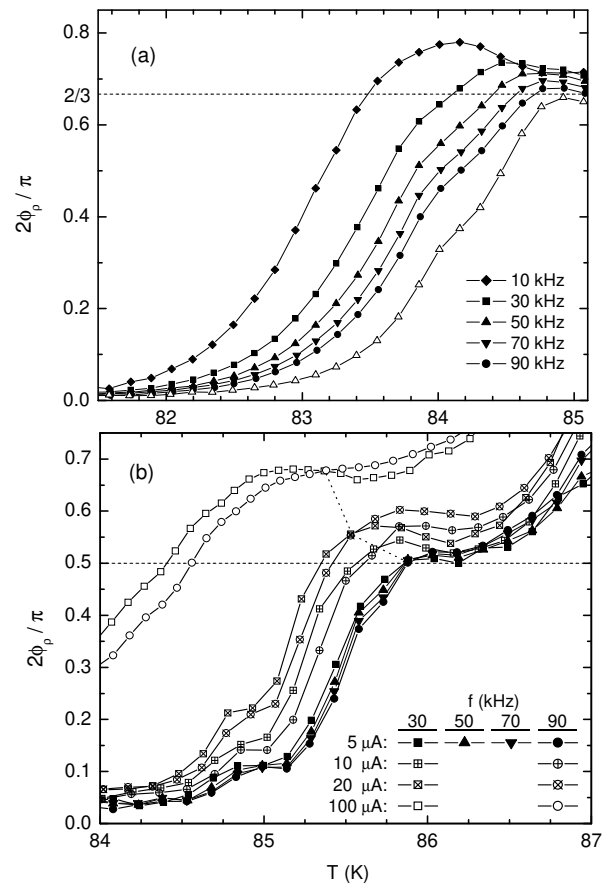


FIG. 3: Normalized phase angle, $2\phi_\rho/\pi$, of the superfluid density extracted from linear response theory. Panel a: $2\phi_\rho/\pi$ in film B taken at $I = 100 \mu A$ (filled symbols) at a series of frequencies and $I = 50 \mu A$ for $f = 50$ kHz (unfilled triangles). Panel b: $2\phi_\rho/\pi$ in film C for a given table of frequencies and drive currents.

film did not show a critical phase angle.

Both the phase angle and the superfluid density is found to be dependent on the drive current near T_c . In the limit of smaller currents, the frequency independent critical phase angle does indeed yield a dynamic exponent of $z = 2.0$. This is a result consistent with the presence of 3D fluctuations. This is also consistent with the behavior of the superfluid density with decreasing current, at fixed frequency, where it is seen to approach the asymptotic static scaling law. Furthermore, the smooth evolution of the phase angle, suggests that the crossover to the two dimensional regime near T^* , is not resolved in our experiment. Nevertheless, the fact that nonlinear scaling and dimensional crossover is expected close to T_c , we now proceed to analyse the nonlinear response, to get a more accurate determination of the dynamic exponent.

Nonlinear scaling: The field equation governing the vector potential, \vec{A} , is

$$\nabla^2 \vec{A}/\mu_0 = -\vec{J}_d - h\delta(z)\sigma\vec{E} \quad (1)$$

where \vec{J}_d is the current density in the drive coil, σ is the conductivity of the superconducting film, and \vec{E} is the electric field. For the geometry of the setup,

$$\vec{J}_d = I_d \delta(r - r_c) \delta(z - z_c) \hat{\phi} \quad (2)$$

in cylindrical coordinates, where I_d is the drive current, r_c is the radius of the drive coil and z_c is the distance from the film to the drive coil [14]. For an anisotropic system, in the critical regime, the superfluid density, ρ , scales as,

$$\rho \sim i\omega\sigma \sim \xi_{ab}^{3-D} \xi_c^{-1} f(i\omega\xi_{ab}^z, E\xi_{ab}^{1+z}) \quad (3)$$

where ξ_{ab} and ξ_c are the correlation lengths parallel and perpendicular to the CuO bilayers, and f is a scaling function. We can non-dimensionalize the equation by rescaling lengths by h , and quantities A and I_d by $(i\omega\xi_{ab}^{1+z})^{-1}$. The solution then takes the form,

$$A = (i\omega\xi_{ab}^{1+z})^{-1} G(i\omega\xi_{ab}^z, i\omega\xi_{ab}^{1+z} I_d, h^2 \xi_{ab}^{3-D} \xi_c^{-1} \Lambda^{-1}, r/h) \quad (4)$$

where G is a function that can be determined by solving the full non-linear field equation and Λ is the thermal length given by $\Phi_0^2/(4\pi\mu_0 k_B T)$. Close to T_c in $D = 3$, using the 3D-XY behavior of the correlation length and the definition of T^* , we can rewrite $h^2 \xi_{ab}^{3-D}/\xi_c$ as,

$$h^2 \xi_{ab}^{3-D}/\xi_c = h |1 + (T - T^*)/(T^* - T_c)|^\nu \quad (5)$$

For a temperature range $|T - T^*| \ll |T^* - T_c|$, $h^2/\xi_c \approx h$. Thus, for temperatures within 0.05K, 0.02K, and 0.01K of T^* for films a, b, and c respectively, this approximation is valid, and the field in Eqn. 4 is a function of only two variables for a given geometry. In this regime we can eliminate ξ_{ab} from Eqn. 4 so that $A = \omega^{1/z} \tilde{G}(I\omega^{-1/z}, h\Lambda^{-1}, r/h)$. The mutual inductance, M , is related to the vector potential at the pick up coil and scales as $M \sim \tilde{G}(I_d i\omega^{-1/z})$, for a given geometry. From our analysis we conclude that the T_c is within 0.02 K of the temperature at which we observe data collapse for film B and C. Within the resolution of our data, any data collapse observed is a 3D phenomena starting to crossover to the asymptotic 2D scaling. It is indeed true that the elimination of the dependence of ξ_{ab} in Eqn. 4 is possible only at T_c and need not hold in the entire regime where the crossover occurs. It is tempting to interpret the experimental results in terms of a two dimensional system. Our data on the other hand are unable to resolve the crossover regime, and yet does exhibit data collapse (see Fig 4). This suggests that the temperature at which we observe data collapse lies in the crossover regime, but is not necessarily the true T_c . We now look for data collapse of our data measured by varying frequency, current and temperature.

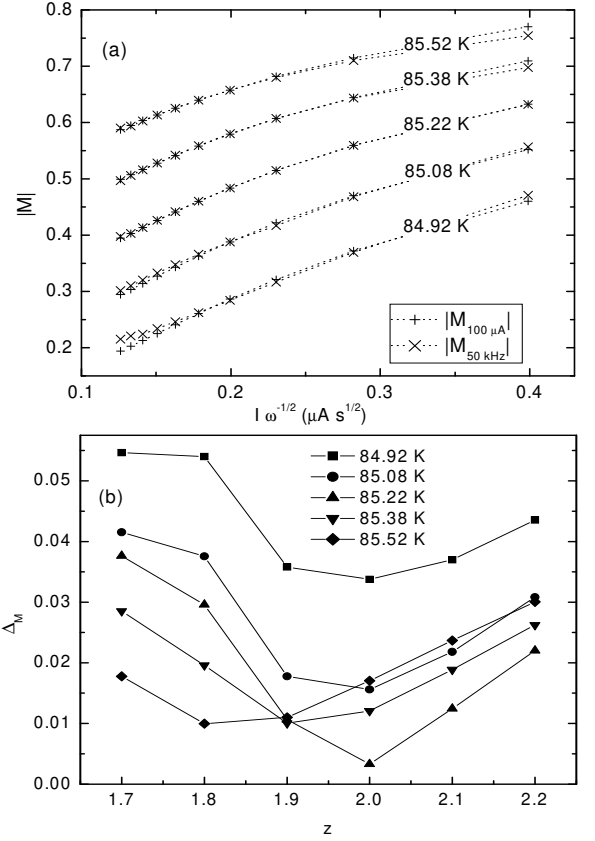


FIG. 4: Panel a: $|M|$ measured at $I = 100 \mu\text{A}$ and $f = 50 \text{ kHz}$ versus the scaling variable $I\omega^{-1/2}$. Panel b: Scaling error at different temperatures versus z .

For the scaling analysis at T_c , the mutual inductance at fixed frequency, M_f , was compared to the mutual inductance at fixed current, M_I . Values of M_f (M_I), were measured at 12.5 μA (10 kHz) intervals for a set of fixed temperatures. Then values of $|M_f|$ were compared with values of $|M_I|$ taken at the same temperature by fitting the raw data of $|M_f|$ to a polynomial and selecting points with the values of $I\omega^{-1/z}$ equivalent to those of $|M_I|$. In Fig. 4(a) $|M_f|$ and $|M_I|$ for film B are plotted versus $I\omega^{-1/2}$ for a series of temperatures. The best agreement between the curves is found to be $z = 2.0$ at $T = 85.22 \text{ K}$. To quantify the fit, in Fig. 4(b), the error in the scaling, Δ_M , for different temperatures and values of z is obtained from $\Delta_M^2 = \sum (|M_f| - |M_I|)^2$, where the sum runs over the 10 values of $I\omega^{-1/z}$ measured for $|M_I|$. The lowest error value indicates $z = 2.0 \pm 0.1$ and $T = 85.2 \pm 0.1 \text{ K}$. A similar analysis for the film C yields $z = 1.8 \pm 0.2$ and $T = 85.9 \pm 0.2 \text{ K}$, which is also consistent with $z = 2.0 \pm 0.1$. The transition temperature of film B is $T_c = 85.2 \pm 0.1 \text{ K}$, while for film C it is $T_c = 85.9 \pm 0.2 \text{ K}$. These values of T_c are close to those obtained with the phase angle measurements.

In Fig. 4(b), the evolution of the error for a fixed trial z , also suggests that the dynamic exponent observed is

indeed due to 3D fluctuations. Notice that as the temperature is increased for $z = 2.0$, the error decreases, approaching the best fit (i.e. data collapse), and then increases again. Within the resolution of the data, we never observe any change to the 2D regime. In other words, the approximation that allowed us to look for the data collapse, is indeed supported by the behavior of the mutual inductance.

Conclusions: The superfluid density in BSCCO films with different thicknesses has been measured and shown to be consistent with the predictions of the 3D-XY model. The dynamic scaling exponent has been obtained by performing both a linear and non-linear scaling analysis. While the linear scaling analysis did yield a 3D dynamic exponent of $z = 2.0$, non-linear effects needed to be stud-

ied to get an accurate determination. This is evident from the current dependence of the critical phase angle of the superfluid density. Similarly, the 3D non-linear scaling analysis yields a dynamic exponent of $z = 2.0 \pm 0.1$.

Acknowledgments

We thank H. Westfahl and D. Sheehy for many helpful discussions. This work was partially supported by the Department of Energy under grant number DEFG02-96ER45439 and the National Science Foundation under grant number NSF-DMR-99-70690.

-
- [1] S. Kamal, D.A. Bonn, N. Goldenfeld, P.J. Hirshfeld, R. Liang, and W.N. Hardy, Phys. Rev. Lett. **73**, 1845 (1994). S. Kamal, R. Liang, A Hosseini, D.A. Bonn, and W.N Hardy, Phys. Rev. B **58**, R 8933 (1998).
 - [2] J.T. Kim, N. Goldenfeld, J. Giapintzakis and D.M. Ginsberg, Phys. Rev. B **56**, 118 (1997).
 - [3] J.C. Booth, D.H. Wu, S.B. Qadri, E.F. Skelton, M.S. Osofsky, A. Pique, and S.M. Anlage, Phys. Rev. Lett. **77**, 4438 (1996).
 - [4] S.M. Ammirata, M. Friesen, S.W. Pierson, L.A. Gorham, J.C. Hunnicutt, M.L. Trawick and C.D. Keener, Physics C **313**, 225 (1999). S.W. Pierson, M. Friesen, S.M. Ammirata, J.C. Hunnicutt and L.A. Gorham, Phys. Rev. B. **60**, 1309 (1999).
 - [5] J. Kotzler and M. Kaufmann, Phys. Rev. B **56**, 13734 (1997).
 - [6] J. Corson, R. Mallozzi, J. Orenstein, J.N. Eckstein, and I. Bozovic, Nature **398**, 221 (1999).
 - [7] P. Minnhagen, Rev. Mod. Phys. **59**, 1001 (1987).
 - [8] S.H. Han, Y. Eltsev and O. Rapp, Jour. Low. Temp. Phys. **117** 1259 (1999). S.H. Han, Y. Eltsev and O. Rapp, Phys. Rev. B. **61**, 11776 (2000).
 - [9] V. Aji and N.D. Goldenfeld, Phys. Rev. Lett **87**, 197003 (2001).
 - [10] P.C. Hohenberg and B.I. Halperin, Rev. Mod. Phys. **49**, 435 (1977).
 - [11] A.T. Fiory, A.F. Hebard, P.M. Mankiewich and R.E. Howard, Phys. Rev. Lett. **61** 1419 (1988).
 - [12] Z.H. Lin, G.C. Spalding, A.M. Goldman, B.F. Bayman, and O.T. Valls, Europhys. Lett. **32**, 573 (1995). K.M. Paget, B.R. Boyce, and T.R. Lemberger, Phys. Rev. B **59**, 6545 (1999).
 - [13] J.N. Eckstein, I. Bozovic, K.E. von Dessonneck, D.G. Schlom, J.S. Harris Jr., and S. M. Baumann Appl. Phys. Lett. **57**, 931 (1990).
 - [14] J.R. Clem and M.W. Coffey, Phys. Rev. B **46**, 14662 (1992).
 - [15] A.T. Fiory, A.F. Hebard, P.M. Mankiewich, and R.E. Howard, Appl. Phys. Lett. **52**, 2165 (1988).
 - [16] S.J. Turneaure, E.R. Ulm, and T.R. Lemberger, J. Appl. Phys. **79**, 4221 (1996). S.J. Turneaure, A.A. Pesetski, T.R. Lemberger, Jour. Appl. Phys. **83**, 4334 (1998).
 - [17] D.S. Fisher, M.P.A. Fisher and D.A. Huse, Phys. Rev. B **43** 130 (1990).
 - [18] M.R. Beasley, J.E. Mooij and T.P. Orlando, Phys. Rev Lett **42**, 1165 (1979).
 - [19] A.T. Dorsey, Phys. Rev. B **43**, 7575 (1991).